Structure and Thermal Denaturation of Crystalline and Noncrystalline Cytochrome Oxidase as Studied by Infrared Spectroscopy†

José L. R. Arrondo,*,‡ José Castresana,§ José M. Valpuesta,‖ and Félix M. Goñi‡

Departamento de Bioquímica, Universidad del País Vasco, Aptdo. 644, E-48080 Bilbao, Spain, European Molecular Biology Laboratory, Meyerhofstrasse 1, D-6900 Heidelberg, Germany, and Centro Nacional de Biotecnología, Universidad Autónoma de Madrid, E-28049 Madrid, Spain

Received January 12, 1994; Revised Manuscript Received June 21, 1994®

ABSTRACT: Fourier-transform infrared spectroscopy has been applied to the study of lipid vesicle-supported two-dimensional crystals and noncrystalline preparations of beef heart cytochrome oxidase. At room temperature, no conformational differences are seen between the noncrystalline and crystalline proteins, whose conformation is shown to consist of ca. 40% α-helix, 20% extended structures (including β-sheet), 17% β-turns, and 22% open loops plus nonstructured conformations. A novel infrared approach that combines quantitative spectral band decomposition with the study of the thermal behavior of each component has been applied. The procedure allows the independent examination of temperature-induced changes in individual structural elements (α-helix, β-sheet, β-turns, and unordered). All these reflect, upon heating the protein from 20 to 80 °C, a major irreversible thermal event centred at 55–60 °C, leading to a molecular state devoid of enzyme activity but with a defined secondary structure; in addition, when the band position, percent area (integrated intensity), and bandwidth of the various amide I components are separately plotted versus temperature, each component is seen to behave in a characteristic way. Thermal denaturation in D_2O buffer shows a decrease in nonstructured conformations and an increase in β-turns without major changes in the proportion of α-helix. Temperature-induced changes are not the same in amorphous and crystalline structures, the latter being in general more stable toward the thermal challenge. The above data extend and confirm previous structural studies on cytochrome oxidase using cryo-electron microscopy.

Cytochrome oxidase (EC 1.9.3.1), the terminal catalyst of the mitochondrial respiratory chain, is an integral membrane protein complex consisting, when isolated from beef heart, of 12–13 different polypeptides (Capaldi et al., 1983b; Valpuesta & Barbon, 1988; Grdadolnik & Hadzi, 1993) with a minimum combined molecular mass of ≈200 kDa. Because of the large size of the complex and the lack of available three-dimensional crystals, cytochrome oxidase is not amenable at present to X-ray diffraction or nuclear magnetic resonance studies. The structure of dimeric cytochrome oxidase in two-dimensional vesicle crystals has been described by cryo-electron microscopy at 10-Å resolution (Valpuesta et al., 1990); a substantial part of the protein appears to be embedded in the lipid bilayer, while most of the remaining portion of the molecule extends into the internal space within the vesicle.

Infrared spectroscopy has shown its potential in the elucidation of protein conformation (Haris & Chapman, 1993), and in spite of its present limitations at the level of structural resolution, it can be applied to both crystalline and noncrystalline preparations of proteins, even of large molecular mass. Infrared spectroscopy has been shown to be sensitive to changes at the single residue level (Rothschild, 1992). The infrared amide I band in the 1600–1700-cm^{-1} region, originating mainly from C=O stretching vibrations of peptide bonds (Krimm & Bandekar, 1986), is the most commonly used band in protein structural studies. The overall appearance of the amide I band is rather featureless, and until the development of band-narrowing techniques, i.e., Fourier deconvolution and derivation, and suitable iterative methods, its applicability has been limited. Nevertheless, recent advances in computer software as well as improvements in instrumentation have dramatically widened the possibilities of quantitative infrared spectroscopy. The various quantitative methods and their respective merits and drawbacks have been recently reviewed (Arrondo et al., 1993).

Infrared studies have been carried out in buffers containing H_2O or D_2O. In H_2O medium, the strong water absorption signal overlapping the amide I band (Fringeli & Günthard, 1981) makes it difficult to obtain a good signal-to-noise ratio, and even if this is achieved, the bands corresponding to α-helical structures and unordered conformations overlap each other (Arrondo et al., 1993). In turn, in D_2O solutions the exchange may not be complete as indicated by a residual amide II band, transmembrane α-helices being resistant to H/D exchange (Earnest et al., 1990). Therefore, a combination of spectra in both media is analyzed in studies from our and other laboratories (Arrondo et al., 1989; Fabian et al., 1992; He et al., 1991).

In the present work, we have applied an improved method of analysis of Fourier transform infrared (FT-IR) spectra to the study of cytochrome oxidase structure. Membrane vesicles containing either native (noncrystalline) or two-dimensional crystalline cytochrome oxidase have been comparatively studied using spectra recorded over the 20–80 °C temperature range. Our data provide quantative information on the enzyme structure that can be matched with the previous electron microscopic observations. The noncrystalline and crystalline forms of the enzyme appear to have similar structure at room temperature; however, differences are detected at the higher temperatures in specific structural components.

† This work was supported in part by funds from University of the Basque Country (Grant 161/92) and DGICYT (Grant PB91-0441).

* Corresponding author.
‡ Universidad del País Vasco.
§ European Molecular Biology Laboratory.
‖ Universidad Autónoma de Madrid.

® Abstract published in *Advance ACS Abstracts,* September 1, 1994.

0006-2960/94/0433-11650$04.50/0

MATERIALS AND METHODS

Cytochrome oxidase was purified from beef heart mitochondria and obtained either in native form or in two-dimensional crystals as described by Valpuesta et al. (1990), following essentially the procedure by Frey et al. (1978). The purified enzyme is obtained in the form of closed vesicles of lipid composition similar to that of the original membrane. The crystalline samples (at least 90% crystallinity as judged by electron microscopy) consist of enzyme dimers, oriented inside-out with respect to the mitochondrial inner membrane. Cytochrome oxidase activity measurements were carried out essentially according to Sinjorgo et al. (1986); specific activities at room temperature were 400 mol of oxidized cytochrome *c* min^{-1} (mol of enzyme)$^{-1}$ for the crystalline sample and 420 mol of oxidized cytochrome *c* min^{-1} (mol of enzyme)$^{-1}$ for the noncrystalline preparation.

All samples for FT-IR were prepared in both H_2O and D_2O buffers (10 mM phosphate, pH or pD 7.0). D_2O substitution, sample treatment, spectra acquisition, and resolution enhancement were performed as described previously (Arrondo et al., 1987; Muga et al., 1993). The protein concentration was ≈40 mg/mL (≈0.2 mM). Quantitative information on protein structure was obtained through decomposition of the amide I band into its constituents. The method used was an improvement of the one described earlier (Castresana et al., 1988; Arrondo et al., 1989). The major differences in the initial estimations were that the baseline was removed before the fitting procedure was started and that initial heights were set at 90% of those in the original spectrum for the bands in the wings and for the most intense component and at 70% of the original intensity for the other bands (Abott et al., 1991). The improved curve-fitting procedure was accomplished in three steps: (i) the band shape of the component bands was fixed at 0.1 Gaussian fraction together with the band position, allowing widths and heights to approach final values; (ii) the Gaussian fraction was left free; and (iii) band positions were left to change. Band decomposition was performed using CURVEFIT running under SpectraCalc (Galactic Inc., Salem, NH). In order to test our method, the parameters obtained were used to construct artificial curves, and it was seen that the three-step procedure gave differences of less than 1% in band areas after the artificial spectra were submitted to the curve-fitting procedure. Also, spectra from well-characterized proteins, i.e., myoglobin and concanavalin A, were subjected to the procedures described with excellent agreement to published data. The use of asymmetric band shapes such as log-normal or Pearson VII did not improve the results.

To study the effect of temperature, samples in D_2O buffer were heated in steps of around 4 °C in the interval 20–80 °C. After every heating step the sample was left to stabilize for 5 min, and the corresponding spectrum was recorded and treated as described above. Measurements in H_2O buffer require longer acquisition times, and the samples may become dehydrated more easily than in D_2O buffer because of the smaller path lengths used; consequently, the heating steps were 10 °C in H_2O medium.

RESULTS

Studies at Room Temperature. The amide I band decomposition of native (noncrystalline) and crystalline cytochrome oxidase is shown in Figure 1. The number and initial position of the component bands were obtained from band-narrowed spectra by Fourier deconvolution and derivation as described (Castresana et al. 1988). Values corresponding to band position, bandwidth, and percentage area obtained from the spectra in Figure 1 (in D_2O buffer) and from similar spectra in H_2O buffer (not shown) are given in Table 1. The spectra in H_2O exhibit nine component bands in the 1700–1600-cm^{-1} region of both native and crystalline cytochrome oxidase, while eight component bands are found in the D_2O spectra of both. The divergence of component areas between noncrystalline and crystalline cytochrome oxidase is ≤2% in all cases, except for a 3% difference in the 1624-cm^{-1} band in D_2O.

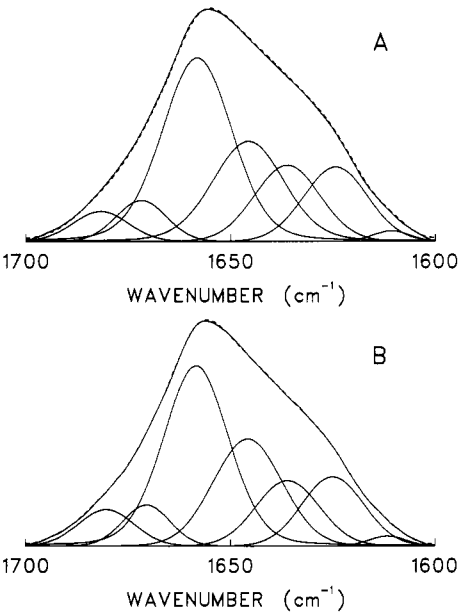

FIGURE 1: Amide I band decomposition. Noncrystalline (A) and crystalline (B) cytochrome oxidase in D_2O buffer are shown. The numerical values obtained are reflected in Table 1.

The assignment of the amide I component bands to conformational structures seems at first difficult since the number of bands is larger than the number of expected secondary structures, and also because natural proteins do not always exhibit the same behavior as model molecules and homopolypeptides that are thought to reflect these secondary structures (Surewicz et al., 1993). Still, some of the bands can be unambiguously assigned, whereas for others reasonable approximations can be made by comparison with data from other techniques (Arrondo et al., 1993). Thus, the band around 1658 cm^{-1} corresponds to α-helix plus nonstructured peptide in H_2O but only to α-helix in D_2O. β-Turns are located between 1665 and 1690 cm^{-1}, whereas the extended structures (β-strands) give rise to signals in the region 1620–1640 cm^{-1}. Two different bands are seen in this region, one around 1636 cm^{-1}, arising clearly from intramolecular C=O vibrations of β-sheets, and one around 1625 cm^{-1}. The latter was first described in homopolypeptides (Susi, 1969) and is also found in denatured proteins in D_2O buffer (Naumann et al., 1993; Muga et al., 1993). However, it is not so common in native proteins in H_2O or D_2O. In proteins, it was first found in concanavalin A (Arrondo et al., 1988; Alvarez et al., 1987) and was assigned to peptides in an extended configuration, with a hydrogen-bonding pattern formed by peptide residues not taking part in intramolecular β-sheet but rather hydrogen-bonded to other molecular structures, e.g., forming intermolecular hydrogen bonding in monomer–monomer interaction. It was also found in triosephosphate isomerase (Castresana et al., 1988), where it is hydrogen-bonded to the α-helix, and even at lower frequency in human low-density lipoproteins,

Table 1: Values Corresponding to Peak Position, Bandwidth, and Percentage Area Obtained after Decomposition of the Amide I Band of Cytochrome Oxidase in Its Noncrystalline or Crystalline Form, Measured in H_2O and D_2O Media

H_2O						D_2O					
noncrystalline			crystalline			noncrystalline			crystalline		
position[a] (cm^{-1})	width[b] (cm^{-1})	area[c] (%)	position[a] (cm^{-1})	width[b] (cm^{-1})	area[c] (%)	position[a] (cm^{-1})	width[b] (cm^{-1})	area[c] (%)	position[a] (cm^{-1})	width[b] (cm^{-1})	area[c] (%)
1690.0	10	1	1691.0	9	1	1693.4	7	<1	1692.0	6	<1
1683.5	19	5	1683.3	18	6	1681.9	16	5	1681.7	16	5
1674.7	21	12	1673.8	20	11	1672.0	15	6	1672.1	14	5
1657.5	21	45	1658.1	22	44	1658.4	21	39	1658.6	21	41
1643.5	18	17	1643.4	19	18	1645.8	21	22	1645.5	23	22
1635.9	16	7	1636.6	18	7	1636.2	19	15	1636.3	21	16
1626.7	17	13	1627.9	20	14	1624.3	19	14	1624.1	18	11
1614.6	14		1613.8	12		1610.7	10		1610.9	9	
1608.3	7		1607.0	6							

[a] Peak position of the amide I band components. [b] Half bandwidth of the amide I components (rounded off to the nearest integer). [c] Percentage area of the band components of amide I. The areas corresponding to side-chain contributions located at 1615–1600 cm^{-1} have not been considered. The values are rounded off to the nearest integer.

where it was assigned to "low-frequency β-sheets" (Goormaghtigh et al., 1989) or to a β-structure less accessible to the external solution (Herzyk et al., 1987). We called this pattern "β-edge" as typical of the outer strands of β-sheets (Arrondo et al., 1988; Castresana et al., 1988); it also implies intermolecular hydrogen bonding, as postulated for the low-frequency bands in irreversibly aggregated proteins (Jackson et al., 1991; Surewicz et al., 1990), or in monomer–monomer contacts, as in concanavalin A (Arrondo et al., 1988). The band near 1643 cm^{-1} has been assigned in D_2O to nonstructured conformations (Susi et al., 1967); however, this assignment appears to be incomplete since the band is also found in H_2O (Fabian et al., 1992), in proteins or peptides with a high amount of 3_{10}-helix (Miick et al., 1992; Prestrelski et al., 1991), and in cyclic peptides (Perczel et al., 1993). The combination of H_2O and D_2O spectra should allow the quantitation of unordered structure, but it is not so conclusive with respect to the amount of "open loops" (fully hydrated, not interacting with nearby amide functional groups) (Fabian et al., 1992) or to any 3_{10}-helix present, although the latter is not usually found in large proportions in membrane proteins. In general, for intrinsic membrane proteins, it can be safely assumed that the 1643-cm^{-1} band contains mainly contributions from nonstructured conformations, including open loops. Thus, secondary structure of cytochrome oxidase obtained from Table 1 is 40% α-helix, 20% extended structures (including β-sheet), 17% β-turns, and 22% loops and nonstructured conformation.

Studies as a Function of Temperature. Protein thermal denaturation profiles are sensitive tools revealing minor conformational differences that are not always apparent from the individual infrared spectra and do not always produce significant changes in enzyme activity (Fernandez-Ballester et al., 1992; Muga et al., 1993). Figure 2 shows a typical pattern of protein thermal denaturation; the prominent bands at around 1682 and 1620 cm^{-1} observed after the thermal event (above ≈55–60 °C) are characteristic of protein aggregation produced after irreversible thermal denaturation and have been described for both soluble and membrane proteins (Muga et al., 1993; Naumann et al., 1993; Jackson et al., 1991; Surewicz et al., 1990). In our preparations, heating above 60 °C leads to a complete and irreversible loss of enzyme activity. Also above that temperature, electron microscopy reveals the disappearance of crystalline arrays and the presence in all samples of extensive vesicle aggregation and collapse of the bilayer structure (data not shown).

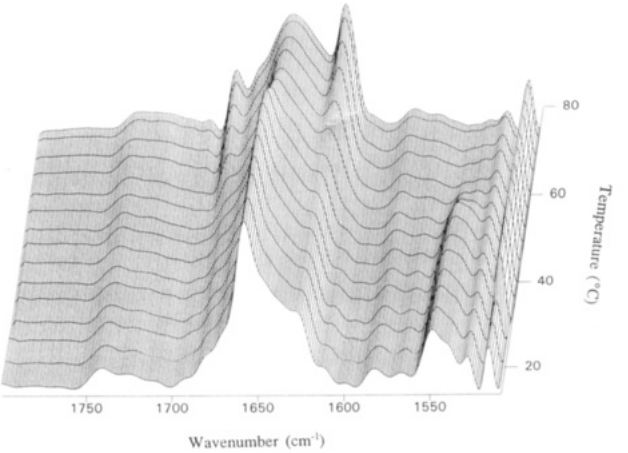

FIGURE 2: Deconvolved spectra corresponding to the region 1800–1500 cm^{-1} (bandwidth = 18 cm^{-1}; $K = 2$) of noncrystalline cytochrome oxidase in D_2O buffer at different temperatures. The z-axis corresponds to temperature.

In order to study the thermal behavior of cytochrome oxidase structural features, the spectra at different temperatures have been decomposed into their constituents by curve-fitting, and the peak positions, widths, and percent areas (integrated intensities) of each component have been plotted as a function of temperature. Again amorphous and crystalline enzyme preparations have been used. As stated in Materials and Methods, spectra in D_2O buffer have been analyzed throughout the temperature range; in addition, spectra in H_2O buffer have been examined at some temperatures. Of the eight band components detected in D_2O (Table 1), the one at 1693 cm^{-1}, which makes up less than 1% of the total band area, and the one at 1611 cm^{-1}, assigned to Tyr side chains, have not been considered.

All six bands under study (positions at room temperature ≈ 1682, 1672, 1658, 1646, 1636, and 1624 cm^{-1}) show some clear thermal effect in either position, area, or bandwidth with a midpoint in the 55–60 °C region (Table 2). However, each of the band components displays a behavior of its own. To mention but two representative examples, the α-helix component (Figure 3) is characterized by a sharp shift in position and gradual increase in bandwidth. In turn, in the intermolecular β-strands (β-edge) (Figure 4) the band shift is not accompanied by an increase in width, but the percent band area is seen to increase incrementally with temperature. Note that, in protein samples equilibrated in D_2O buffer at room temperature, a complete H/D exchange is not produced

Table 2: Summary of the Temperature-Induced Changes in the Components of the Cytochrome Oxidase Infrared Spectrum Amide I Band

band position[a]	main assignment	shift in position		change in % area		change in bandwidth	
		break[b]	range[c] (cm^{-1})	break[b]	range[c] (%)	break[b]	range[c] (cm^{-1})
1682	β-turns	yes	1685–1682	yes	6–1	yes	15–9
1672	β-turns	no	1671–1672	yes	5–17	yes	13–25
1658	α-helix	yes	1658–1653	no	40–39	no	20–25
1646	nonstructure + loops	no	1646–1643	yes	23–4	yes	20–15
1636	β-sheet	yes	1636–1634 (1636–1636)	no	19–20 (19–25)[d]	no	20–21
1624	intermolecular β-strands (β-edge)	yes[d]	1624–1620	no	12–21 (11–15)[d]	no	20–19

[a] At room temperature. [b] Presence or absence of a thermally induced discontinuity in this parameter at ≈55–60 °C. [c] Change in this parameter on going from 20 to 78 °C. In parentheses are the values for the crystalline sample if different. [d] A difference is detected in the thermal behavior of this particular parameters between the amorphous and crystalline samples.

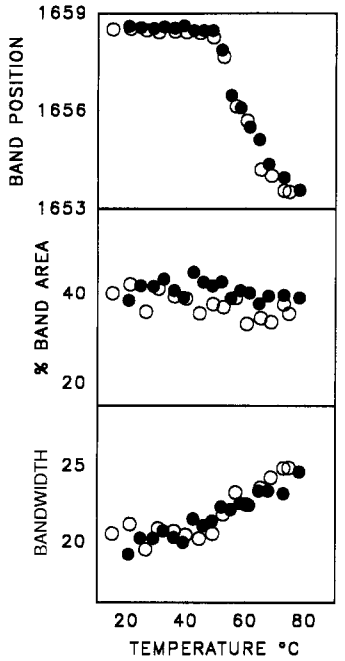

FIGURE 3: Thermal profiles of the amide I component detected (at room temperature) at 1658 cm^{-1} (α-helix). Band position, % band area, and bandwidth are plotted as a function of temperature for the noncrystalline (○) and crystalline (●) preparations of cytochrome oxidase in D_2O buffer.

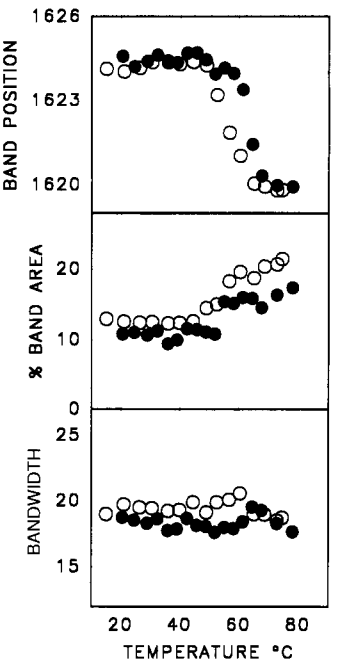

FIGURE 4: Thermal profiles of the amide I component detected (at room temperature) at 1624 cm^{-1} (intermolecular β-strands or β-edge). Band position, % band area, and bandwidth are plotted as a function of temperature for the noncrystalline (○) and crystalline (●) preparations of cytochrome oxidase.

before thermal denaturation takes place. Thus the changes summarized in Table 2 could have a component due to the additional deuteration. Discrimination of the deuteration effect can be accomplished by comparing the spectra of cytochrome oxidase at 80 °C in H_2O and D_2O (Figure 5). The various components detected at room temperature (Table 1) are still present after the heat treatment, and each of them has been modified in a characteristic way. For the most prominent band component, corresponding in H_2O to α-helix plus unordered structures, the changes in percent band area and bandwidth are alike in both media, whereas its position shifts in H_2O from 1657.5 cm^{-1} (at 20 °C) to 1655 cm^{-1} (at 80 °C). This shift is smaller than the one observed in D_2O, suggesting that in the latter case the thermally induced shift is increased by the deuteration effect.

A comparison of the thermal behavior of noncrystalline and crystalline cytochrome oxidase shows that in most cases there appear to be no differences between those preparations, confirming what was seen at room temperature. However, there are at least two instances in which temperature-treated samples show quantitative differences between the crystalline and noncrystalline forms; these are the temperature-induced changes in extended chains, β-sheet, and β-edge (intermolecular hydrogen-bonded β-strands) (Table 3 and Figure 4). In the latter, the temperature at which the thermal event takes place is increased by 6 °C in the crystalline sample, and in the β-sheet band, the change in position observed in the noncrystalline form is prevented in the crystalline sample; in both situations the crystalline sample appears to be relatively more stable.

DISCUSSION

Secondary Structure of Cytochrome Oxidase. Infrared spectroscopy may provide quantitative information on the secondary structure of soluble and membrane proteins in aqueous environments (Haris & Chapman, 1993; Arrondo et al., 1993). In our case, the percent values found for the various secondary structure components are in good agreement with most previous predictions and studies by different techniques. Capaldi et al. (1983a) suggested from predictive studies the existence of 21 transmembrane helices in the beef enzyme consisting of subunits I, II, III, IV, V, VI, VII Ser, and VII Ile; assuming an average length of 22 aa/helix and an average molecular mass of 120 Da/aa residue, this would correspond to ≈34% of amino acids involved in α-helices. Saraste (1990) predicted 21 helices in subunits I, II, and III of *Paracoccus*

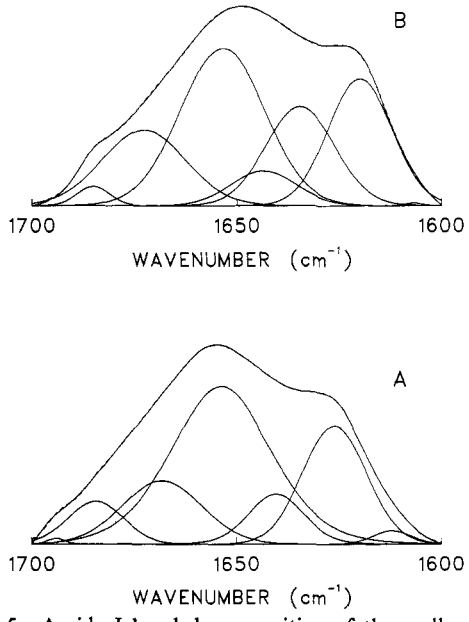

FIGURE 5: Amide I band decomposition of thermally denatured cytochrome oxidase. (A) Sample in H_2O buffer; (B) sample in D_2O buffer. The samples had undergone a heating cycle up to 80 °C.

denitrificans, which amounts to ≈41% α-helix in that enzyme. Valpuesta et al. (1990), from their study of cryo-electron microscopic analysis of beef crystalline cytochrome oxidase, suggested the existence of 12–16 α-helices/monomer, which would correspond to 32–42% α-helix (assuming that the bulk of the hydrophobic region is contributed by subunits I, II, and III). Our own experimental result (40%) is in good agreement with the above figures, particularly in view of the uncertainties in those studies: subunit stoichiometry, validity of predictions, or the existence of extramembranous helical stretches.

Studies based on circular dichroism also provide similar values (37–44%) for the α-helix content (Bazzi & Woody, 1985; Myer, 1971; Park et al., 1992). The same authors estimate the β-sheet contents of cytochrome oxidase at 13–18% (our value 20%) and the proportion of turns at 12–14% (our value 17%). A recent study of the secondary structure of beef heart cytochrome oxidase by infrared spectroscopy (Caughey et al., 1993) puts the α-helix contents at 61%; however, this value cannot be considered as reliable, since it was obtained through decomposition of second-derivative spectra, and it is known that derivatization does not preserve the relative areas of the original spectral components (Surewicz et al., 1993).

Temperature Effects on Cytochrome Oxidase Structure. The band decomposition procedure used in this work allows the analysis of thermally induced changes in protein structure in detail and the thermal behavior of the individual structural elements may be separately followed. In our case, six different secondary structure components have been analyzed (Table 2). For each component, band position, percentage of amide I band area, and bandwidth have been considered. Band position is thought to reflect the conformation of the structural element under study (e.g., α-helix, β-sheet, and so on). To simplify interpretation, it can be stated that, in general, large changes (≥10 cm^{-1}) in band position indicate variations in the secondary structure, whereas smaller shifts (≤6 cm^{-1}) reflect local changes in a given conformation. The integrated intensity of each component, usually expressed as percent band area, can be related to the proportion of peptide in that particular conformation. Finally, the width-at-half-height (often expressed as bandwidth) is related to the freedom of movement of the structure associated with that particular component (Casal et al., 1980).

The onset of thermal effects on cytochrome oxidase structure is detected at ≈45–50 °C. The thermal treatment under our conditions leads to a complete loss of activity after a 20–80 °C heating run. This is in agreement with the differential scanning calorimetry data published by Morin et al. (1990) on the thermal denaturation of membrane-reconstituted noncrystalline yeast cytochrome oxidase. The main structural effects that accompany thermal denaturation are summarized in Table 2; some of them deserve a separate comment. The relative proportions of the various components do not change very much, except for the decrease in the band around 1646 cm^{-1} including unordered structure plus loops, which is virtually absent at 80 °C, and the concomitant increase in the proportion of β-turns. Thermal energy may be used by some peptide regions to attain degrees of structure that are not accessible at room temperature. At high temperatures the protein appears to "break bindings", and this is accompanied by its full deuteration, as seen by the complete loss of he amide II residual band (Figure 2). However, the conformational perturbation produced by temperature cannot always be stabilized within the solvent, and aggregation is produced, as shown by Sosnick and Trewhella (1992), for a modified ribonuclease A. According to our FT-IR observations, thermal denaturation of cytochrome oxidase is accompanied by aggregation. This is compatible with the persistence of native secondary structure components. Such is the case of the α-helix; while shifting its position with temperature, it does not change in percentage area, and its bandwidth follows a small, steady increse, compatible with an increase in mobility produced by the thermal perturbation induced in its environment. This suggests that this conformational component, perhaps embedded in the bilayer, is not drastically modified by temperature.

From a qualitative analysis of the spectra of Figure 2 it could be thought that, after thermal denaturation, the amide I band could be fitted by three bands, the one centered around 1645 cm^{-1}, associated to unordered structure, and the two bands due to aggregation, as found in the methionine aporepressor of *Escherichia coli* (Yang et al., 1987). This is, however, not the case in cytochrome oxidase. Derivative and deconvolved spectra also show other components in the denatured protein that were present in the native state, and attempts to fit the amide I band with only those three components proved unsuccessful (not shown). For samples thermally treated in H_2O buffers, the persistence of structural components after functional denaturation has also been demonstrated (Figure 5). Complex amide I bands containing various secondary structure components have been found by infrared spectroscopy in both soluble and membrane proteins after heat denaturation (Fernandez-Ballester et al., 1992; Sosnick & Trewhella, 1992; Fabian et al., 1993; Urbanova et al., 1993; Seshadri et al., 1994). In a recent study, differential scanning calorimetry and infrared spectroscopy were used in combination to explain the presence of residual secondary structure in a cytochrome oxidase from *Paracoccus* (Haltia et al., 1994).

Crystalline vs Noncrystalline Structures. Three-dimensional protein structures may be obtained either from crystals (e.g., by X-ray diffraction) or from proteins in solution (e.g., by nuclear magnetic resonance). However, structural data obtained by the same technique on both crystal and solution forms of a given protein have not been available up to now. Using infrared spectroscopy, we have examined a protein,

cytochrome oxidase, in two-dimensional crystals as well as in amorphous form. The lack of observable differences between the structures of the crystalline and amorphous preparations at room temperature (Table 1), together with a similar activity in both preparations, is an important result in order to apply structural studies on protein crystals to the physiological noncrystalline situation.

In spite of the above, some differences occur between the crystalline and amorphous samples after the thermal treatment (Table 2). In both β-sheet and β-edge, the crystalline forms are more stable toward the thermal challenge than their noncrystalline counterparts. The structures influenced by the degree of crystallinity appear to be in the extramembranous portion of the enzyme. According to Valpuesta et al. (1990), the vesicles containing crystalline cytochrome oxidase are flattened, so that interaction between the bulky, intravesicular protein domains from opposite faces of the flattened vesicle is facilitated [see Figure 9 of Valpuesta et al. (1990)]. In the crystalline form the "melting point" of the extended β-edge component, as observed by fitting the points to a sigmoid curve through nonlinear correlation, is 6 °C higher than in the amorphous form (Figure 4). Since a decrease in denaturation temperature is associated with a looser protein packing (Arrondo et al., 1988), the observed temperature increment can be attributed to increased protein–protein interactions between opposite bilayers in the collapsed vesicles that support the two-dimensional crystals (Valpuesta et al., 1990; Kühlbrandt, 1992). These interactions, which can effectively modify the thermal properties of certain protein components, are nevertheless unable to produce observable changes in conformation between the crystalline and amorphous forms of the protein at room temperature (Table 1).

REFERENCES

Abott, T. P., Wolf, W. J., Wu, Y. V., Butterfield, R. O., & Kleiman, R. (1991) *Appl. Spectrosc. 45*, 1665.

Alvarez, J., Haris, P. I., Lee, D. C., & Chapman, D. (1987), *Biochim. Biophys. Acta 916*, 5.

Arrondo, J. L. R., Mantsch, H. H., Müller, N., Pikula, S., & Martonosi, A. (1987) *J. Biol. Chem. 262*, 9037.

Arrondo, J. L. R., Young, N. M., & Mantsch, H. H. (1988) *Biochim. Biophys. Acta 952*, 261.

Arrondo, J. L. R., Muga, A., Castresana, J., Bernabeu, C., & Goñi, F. M. (1989) *FEBS. Lett. 252*, 118.

Arrondo, J. L. R., Muga, A., Castresana, J., & Goñi, F. M. (1993) *Prog. Biophys. Mol. Biol. 59*, 23.

Bazzi, M. D., & Woody, R. W. (1985) *Biophys. J. 48*, 957.

Capaldi, R. A., Malatesta, F., & Darley-Usmar, V. M. (1983a) *Biochim. Biophys. Acta 726*, 135.

Capaldi, R. A., Marshall, F. A., & Staples, S. J. (1983b) *Comments Mol. Cell. Biophys. 1*, 365.

Casal, H. L., Cameron, D. G., Smith, I. C. P., & Mantsch, H. H. (1980) *Biochemistry 19*, 444.

Castresana, J., Muga, A., & Arrondo, J. L. R. (1988) *Biochem. Biophys. Res. Commun. 152*, 69.

Caughey, W. S., Dong, A., Sampath, V., Yoshikawa, S., & Zhao, X.-J. (1993) *J. Bioenerg. Biomembr. 25*, 81.

Earnest, T. N., Herzfeld, J., & Rothschild, K. J. (1990) *Biophys. J. 58*, 1539.

Fabian, H., Naumann, D., Misselwitz, R., Ristau, O., Gerlach, D., & Welfle, H. (1992) *Biochemistry 31*, 6532.

Fabian, H., Schultz, C., Naumann, D., Landt, O., Hahn, U., & Saenger, W. (1993) *J. Mol. Biol. 232*, 967.

Fernandez-Ballester, G., Castresana, J., Arrondo, J. L. R., Ferragut, J. A., & Gonzalez-Ros, J. M. (1992) *Biochem. J. 288*, 421.

Frey, T. G., Chan, S. H. P., & Schatz, G. (1978) *J. Biol. Chem. 253*, 4389.

Fringeli, U. P., & Günthard, H. H. (1981) in *Membrane Spectroscopy* (Grell, E., Ed.) pp 270–332, Springer, Berlin.

Goormaghtigh, E., De Meutter, J., Vanloo, B., Brasseur, R., Rosseneu, M., & Ruysschaert, J. M. (1989) *Biochim. Biophys. Acta* 1006, 147.

Grdadolnik, J., & Hadzi, D. (1993) *Chem. Phys. Lipids 65*, 121.

Haltia, T., Semo, N., Arrondo, J. L. R., Goñi, F. M., & Freire, E. (1994) *Biochemistry 33*, 9731.

Haris, P. I., & Chapman, D. (1993) *Biochem. Soc. Trans. 21*, 9.

He, W. Z., Newell, W. R., Haris, P. I., Chapman, D., & Barber, J. (1991) *Biochemistry 30*, 4552.

Herzyk, E., Lee, D. C., Dunn, R. C., Bruckdorfer, K. R., & Chapman, D. (1987) *Biochim. Biophys. Acta 922*, 145.

Jackson, M., Haris, P. I., & Chapman, D. (1991) *Biochemistry 30*, 9681.

Krimm, S., & Bandekar, J. (1986) *Adv. Protein Chem. 38*, 181.

Kühlbrandt, W. (1992) *Q. Rev. Biophys. 25*, 1.

Miick, S. M., Martinez, G. V., Fiori, W. R., Todd, A. P., & Millhauser, G. L. (1992) *Nature 359*, 653.

Morin, P. E., Diggs, D., & Freire, E. (1990) *Biochemistry 29*, 781.

Muga, A., Arrondo, J. L. R., Bellon, T., Sancho, J., & Bernabeu, C. (1993) *Arch. Biochem. Biophys. 300*, 451.

Myer, Y. P. (1971) *J. Biol. Chem. 246*, 1241.

Naumann, D., Schultz, C., Görne-Tschelnokow, U., & Hucho, F. (1993) *Biochemistry 32*, 3162.

Park, K., Perczel, A., & Fasman, G. D. (1992) *Protein Sci. 1*, 1032.

Perczel, A., Majer Z., Holly, S., Machytka, D., Fasman, G. D., & Hollósi, M. (1993) *Tetrahedron: Asymmetry 4*, 591.

Prestrelski, S. J., Ryler, D. M., & Thompson, M. P. (1991) *Int. J. Pept. Protein Res. 37*, 508.

Rothschild, K. J. (1992) *J. Bioenerg. Biomembr. 24*, 147.

Saraste, M. (1990) *Q. Rev. Biophys. 23*, 331.

Seshadri, S., Oberg, K. A., & Fink, A. L. (1994) *Biochemistry 33*, 1351.

Sinjorgo, K. M. C., Steinebach, O. M., Dekker, H. L., & Muijsers, A. O. (1986) *Biochim. Biophys. Acta 850*, 108.

Sosnick, T. R., & Trewhella, J. (1992) *Biochemistry 31*, 8329.

Surewicz, W. K., Leddy, J. J., & Mantsch, H. H. (1990) *Biochemistry 29*, 8106.

Surewicz, W. K., Mantsch, H. H., & Chapman, D. (1993) *Biochemistry 32*, 389.

Susi, H. (1969) in *Structure and Stability of Biological Macromolecules* (Timasheff, S. N., & Stevens, L., Eds.) pp 575–663, Dekker, New York.

Susi, H., Timasheff, S. N., & Stevens, L. (1967) *J. Biol. Chem. 242*, 5460.

Urbanova, M., Pancoska, P., & Keiderling, T. A. (1993) *Biochim. Biophys. Acta 1203*, 290.

Valpuesta, J. M., & Barbon, P. G. (1988) *Biochim. Biophys. Acta 955*, 371.

Valpuesta, J. M., Henderson, R., & Frey, T. G. (1990) *J. Mol. Biol. 214*, 237.

Yang, P. W., Mantsch, H. H., Arrondo, J. L. R., Saint-Girons, I., Guillou, Y., Cohen, G. N., & Barzu, O. (1987) *Biochemistry 26*, 2706.